Large Enhancement of Functional Activity of Active Site-Inhibited Factor VIIa Due to Protein Dimerization: Insights into Mechanism of Assembly/Disassembly from Tissue Factor†

Matthew D. Stone,‡ Stephen B. Harvey,‡ Michael B. Martinez,‡ Ronald R. Bach,§ and Gary L. Nelsestuen*,‡

Department of Biochemistry, Molecular Biology, and Biophysics, University of Minnesota, 6-155 Jackson Hall, 321 Church Street SE, Minneapolis, Minnesota 55455, Veterans Administration Medical Center, 1 Veterans Drive, Minneapolis, Minnesota 55417, and The Department of Medicine, University of Minnesota, 480 Mayo 420 Delaware Street SE, Minneapolis, Minnesota 55455

Received January 3, 2005; Revised Manuscript Received February 22, 2005

ABSTRACT: Active site-inhibited blood clotting factor VIIa (fVIIai) binds to tissue factor (TF), a cell surface receptor that is exposed upon injury and initiates the blood clotting cascade. FVIIai blocks binding of the corresponding enzyme (fVIIa) or zymogen (fVII) forms of factor VII and inhibits coagulation. Although several studies have suggested that fVIIai may have superior anticoagulation effects in vivo, a challenge for use of fVIIai is cost of production. This study reports the properties of dimeric forms of fVIIai that are cross-linked through their active sites. Dimeric wild-type fVIIai was at least 75-fold more effective than monomeric fVIIai in blocking fVIIa association with TF. The dimer of a mutant fVIIai with higher membrane affinity was 1600-fold more effective. Anticoagulation by any form of fVIIai differed substantially from agents such as heparin and showed a delayed mode of action. Coagulation proceeded normally for the first minutes, and inhibition increased as equilibrium binding was established. It is suggested that association of fVIIa(i) with TF in a collision-dependent reaction gives equal access of inhibitor and enzyme to TF. Assembly was not influenced by the higher affinity and slower dissociation of the dimer. As a result, anticoagulation was delayed until the reaction reached equilibrium. Properties of different dissociation experiments suggested that dissociation of fVIIai from TF occurred by a two-step mechanism. The first step was separation of TF−fVIIa(i) while both proteins remained bound to the membrane, and the second step was dissociation of the fVIIa(i) from the membrane. These results suggest novel actions of fVIIai that distinguish it from most of the anticoagulants that block later steps of the coagulation cascade.

Vascular injury results in exposure of anionic phospholipids and the receptor tissue factor (TF)[1] from subendothelial cells. Factor VIIa (fVIIa), a vitamin K-dependent protease that typically comprises about 1% of the total plasma level of factor VII (*1*), specifically recognizes anionic phospholipids (*2*) and binds to TF in a high-affinity interaction (*3*−*7*). Binding to both of these components leads to a large (10^7) enhancement of catalytic efficiency of fVIIa (*8*−*10*). FVIIa catalyzes the activation of factor IX and factor X (fX) to their respective active forms, factor IXa and fXa, thereby triggering the coagulation cascade. Recent studies have shown that TF also circulates in healthy blood in an encrypted form (*11*, *12*). It appears to be recruited to activated platelets in models of clotting (*13*, *14*). Thus, not only does TF initiate clotting but it also could participate in propagation of the response.

Anticoagulation is a critical therapy. Heparin is a commonly used anticoagulant that functions by combination with antithrombin III to enhance its rate of thrombin and factor Xa inhibition. Heparin's action on coagulation is instantaneous. However, heparin can have adverse side effects, and proper dosing can be difficult (*15*−*17*). Active site-inhibited factor VIIa (fVIIai) has 7−10 times higher affinity for TF (*10*, *18*, *19*) than fVIIa. In rat, rabbit, and baboon models, fVIIai was an effective anticoagulant (*20*) with the unique property of inhibiting platelet deposition and lesion formation

† Supported in part by NIH Grants HL60859 and HL65578 (G.L.N.) and by the Merit Review Funding from the Office of Research and Development Medical Research Service, Department of Veterans Affairs.

* Corresponding author. Phone: (612) 624-3622. Fax: (612) 625-2163. E-mail: nelse002@umn.edu.

‡ University of Minnesota.

§ Veterans Administration Medical Center and The Department of Medicine.

[1] Abbreviations: TF, tissue factor; sTF, TF_{1-219}; fVIIa, factor VIIa; fVIIai, active site-inhibited factor VIIa; fVIIa(i), factor VIIai or fVIIa, undesignated; fVIIa-QE, fVIIa-P10Q/K32E; fX(a), factor X(a); PS, phosphatidylserine; PC, phosphatidylcholine; PE, phosphatidylethanolamine; biotinyl-PE, *N*-((6-(biotinoyl)amino)hexanoyl)-1,2-dihexadecanoyl-*sn*-glycero-3-phosphoethanonamine; FPRck, phenylalanylprolylarginyl chloromethyl ketone; FFRck, phenylalanylphenylalanylarginyl chloromethyl ketone; PEG, poly(ethylene glycol); DTPA, diethylenetriaminepentaacetic acid; SBA, succinimidylbutanoate ester; HPLC, high-performance liquid chromatography; S-2238, H-D-phenylalanyl-L-pipecolyl-L-arginine-*p*-nitroaniline dihydrochloride; S-2288, H-D-isoleucyl-L-prolyl-L-arginine-*p*-nitroaniline dihydrochloride; S-2765, Z-D-arginylglycylarginine-*p*-nitroaniline dihydrochloride; TBS, Tris-buffered saline; TBSA, Tris-buffered saline containing bovine serum albumin; $(fVIIai)_2$−PEG, dimeric VIIai with a PEG-3400 cross-linker; $(fVIIai)_2$-DTPA, dimeric VIIai with a DTPA cross-linker.

10.1021/bi050007z CCC: $30.25
Published on Web 03/30/2005

while limiting blood loss (*21*−*24*). It also inhibited sepsis-induced intravascular clotting in baboons (*25*, *26*). Unfortunately, the required dosage is high and may limit the use of fVIIai due to cost of production.

One way to lower cost is to lower the amount of protein needed by improving functional activity. Enhanced function has been produced by mutagenesis of the membrane-binding site. One mutant, fVIIa-P10Q/K32E (fVIIa-QE) had a 25-fold increase of membrane affinity (*27*) and a similar functional change (*18*). Another potential way to improve activity would be to create multimeric proteins that bind simultaneously to several proteins or membrane sites. Multiplying the free energy of binding could produce extremely high affinity and function.

This study describes the properties of dimeric forms of fVIIai that are cross-linked by homobifunctional active site-directed inhibitors. Dimeric forms of fVIIai displayed up to 1600-fold higher function than wild-type monomeric fVIIai. This advantage was observed at binding equilibrium but not in kinetically determined reactions. Consequently, anticoagulation by these agents may offer advantages in some situations and disadvantages in others.

MATERIALS AND METHODS

Proteins. Purified recombinant human fVIIa-wt was obtained from Novo Nordisk (Princeton, NJ). Recombinant human factor VIIa-QE was prepared as described (*28*). TF_{1-219} (sTF) was provided by Dr. Walt Kisiel, University of New Mexico. FVIIai-QE and fVIIai-wt were prepared by adding a 5-fold molar excess of phenylalanylprolylarginyl chloromethyl ketone (FPRck) to fVIIa-QE in Tris-buffered saline (TBS, 50 mM Tris, 100 mM NaCl, pH 7.5) containing 5 mM calcium for 2 h at 22 °C, followed by dialysis to remove remaining inhibitor. Recombinant human TF either was obtained as the reconstituted commercial product, Innovin (Dade Behring, Deerfield, IL), or was purchased as a purified protein from American Diagnostica (Stamford, CT) and reconstituted as described below. Human fX and thrombin were from Enzyme Research Labs (South Bend, IN). Streptavidin (SA) was from Sigma (St. Louis, MO).

Synthesis and Characterization of Bifunctional Cross-Linking Agents. Diethylenetriaminepentaacetic acid (DTPA) dianhydride (Sigma) was mixed in serial additions as a solid to 100 mM HEPES, pH 8.5, containing 40 mM phenylalanylphenylalanylarginyl chloromethyl ketone (FFRck) (Bachem, King of Prussia, PA) to a final concentration of 200 mM. The pH of the reaction solution was monitored and maintained at 8.5 by addition of 1 M NaOH as needed. After 60 min at 22 °C the reaction was complete. Reaction products were separated by reverse-phase high-performance liquid chromatography (HPLC) using a 0.4 × 25 cm Vydac C18 column. Prior to column loading, the reaction solution was adjusted to 0.1% trifluoroacetic acid (TFA). A gradient of 20−24% acetonitrile in 0.1% TFA over 30 min was used to elute the diFFRck product. A peak eluting at 20.8 min was identified as diFFRck−DTPA. It gave a monoisotopic mass of 1358.2 amu in a Finnigan LCQ electrospray mass spectrometer and showed the isotope pattern characteristic of a compound with two chlorine atoms. Acetonitrile was removed, and the bifunctional reagent was concentrated by vacuum centrifugation. The concentration of the reagent was estimated by absorbance at 256 nm using a Beckman DU-70 spectrophotometer and an extinction coefficient of 190 M^{-1} cm^{-1} for the two phenylalanine residues per molecule.

The diFPRck−PEG-3400 cross-linking agent was synthesized from PEG-3400−[succinimidylbutanoate ester (SBA)]$_2$ (final concentration of 5 μM; Shearwater Polymers, Huntsville, AL), which was added stepwise as a solid to 100 mM HEPES buffer at pH 8.0 containing 50 μM phenylalanylprolylarginyl chloromethyl ketone (FPRck) (Bachem). The pH of the reaction solution was monitored and adjusted to 8.0 by addition of 1 M NaOH as needed. The reaction was complete in 60 min at 22 °C. The solution was acidified by addition of TFA to 0.1%. Reaction products were purified by reverse-phase HPLC with a gradient of acetonitrile:water (25:75 to 40:60) containing 0.1% TFA over 15 min. Peaks with significant absorbance at 256 nm were collected and concentrated by vacuum centrifugation. Product concentration was estimated by inhibition of known amounts of thrombin. Briefly, peaks from the HPLC column that contained adducts of FPRck were added to thrombin (0.35 μM) in TBS. The solutions were incubated at 22 °C for 30 min, and the remaining thrombin was measured by chromogenic assay. The thrombin was added to a solution of TBS with 0.1% bovine serum albumin (TBSA) and 150 μM H-D-phenylalanyl-L-pipecolyl-L-arginine-*p*-nitroaniline dihydrochloride (S-2238) (Chromogenix, West Chester, OH). Absorbance change per minute at 405 nm was recorded with a Beckman DU-70 spectrophotometer. Comparison to absorbance change produced by an unmodified thrombin solution allowed estimation of the concentration of FPRck in the fraction. The peak containing the homobifunctional reagent was identified by its ability to cross-link thrombin. Thrombin inhibition reactions from each peak of the HPLC elution were separated in nonreducing SDS−PAGE using a 10% gel that was stained with Bio-Safe Coomassie blue (SDS−PAGE reagents were from Bio-Rad, Hercules, CA). A band migrating with an apparent molecular mass of 75 kDa indicated dimeric thrombin. From this analysis, the peak eluting from the HPLC column at 13.5 min was identified as the bifunctional active site-directed reaction product, diFPRck−PEG-3400.

Production of Dimeric FVIIai. FVIIa-wt was first separated from stabilizers present in the commercial product by application to an ion- exchange column (Mono-Q) (Amersham Pharmacia, Uppsala, Sweden) that was washed with 15 column volumes of 50 mM Tris and 50 mM NaCl, pH 7.5, buffer. The protein was eluted in the same buffer containing 500 mM NaCl and dialyzed overnight at 4 °C against TBS.

Half molar equivalents of the appropriate bifunctional reagent were added to fVIIa (0.1−0.6 μM) in TBS containing 5 mM calcium. Reactions with diFFRck−DTPA were aided by inclusion of phospholipid vesicles [phosphatidylserine (PS):phosphatidylcholine (PC), 20:80; phospholipids:protein, 1.5:1.0 (w/w)]. The phospholipids were large unilamilar vesicles prepared by extrusion and quantified as described (*29*). Reactions were incubated at room temperature for at least 4 h. Reaction progress was monitored in either a one- or two-stage amidolytic assay similar to that described above. For the one-stage assay, a small aliquot was incubated in TBS with 5 mM calcium containing 100 nM sTF. Remaining fVIIa activity was measured by absorbance change at 405

nm per minute after addition of H-D-phenylalanyl-L-pipecolyl-L-arginine-*p*-nitroaniline dihydrochloride (S-2288) (Chromogenix) to 200 μM. For the two-stage assay, an aliquot was incubated in TBS with 5 mM calcium containing Innovin at saturating concentration (estimated to be 0.5 nM) for 5 min at 37 °C. FX (100 nM) was added and the mixture incubated for 60 s. The reaction was quenched with addition of EDTA (12 mM). The amount of fXa formed in the first stage was measured by absorbance change at 405 nM after addition of 200 μM Z-D-arginylglycylarginine-*p*-nitroaniline dihydrochloride (S-2765) (Chromogenix). If significant activity remained, appropriate amounts of the bifunctional reagent were added, and the solution was incubated overnight. The reaction was complete when <1% of original fVIIa activity remained. For reactions with diFPRck−PEG-3400, all remaining fVIIa was inhibited by addition of 1 mM diisopropyl fluorophosphate (Sigma) for 2 h at 22 °C. For the diFFRck−DTPA reactions, remaining VIIa was inhibited by addition of FFRck at a ratio of 2:1 (FFRck:fVIIa). Two hours at 22 °C completed the reaction. EDTA was added to dissociate the protein from vesicles, which were then removed from the protein by gel filtration on Sephadex G-100 (Sigma). The vesicles eluted first and the dimeric protein at the leading edge of the protein peak. Fractions from the leading edge of the protein peak were collected. Protein concentrations for all preparations were determined by Bradford analysis using the protein assay reagents and procedure from Bio-Rad. The standard was fVIIa-wt.

SDS−PAGE of Dimeric Proteins. Proteins were resolved as described above for thrombin. After staining with Bio-Safe Coomassie blue, relative amounts of protein in the different bands were estimated by densitometric analysis with Kodak imaging software. Individual bands were selected, and background pixelation was subtracted. The yield of dimeric protein was calculated as the percentage of protein migrating in a double band at approximately 97 kDa divided by total protein in all bands.

Equilibrium Competition Assays. The assay was essentially that described in ref *28*. Briefly, 20 or 100 nM fVIIa-QE was added to 4 or 18 pM TF (provided by diluted Innovin in TBSA) and 5 mM calcium. FVIIai or dimeric fVIIai was added to various levels. The reactions were mixed and incubated for 60 min at 37 °C to reach equilibrium. FX was added to 100 nM and incubation continued for 5 or 10 min. The reaction was quenched by addition of EDTA to 12 mM. FXa activity was measured by chromogenic assay as described above.

The fraction of TF bound to VIIa (VIIa−TF) was calculated by comparison of fXa generated in the inhibited reaction to that generated in a reaction that contained no inhibitor [(fVIIa−TF) = fXa with inhibitor/fXa without inhibitor]. The fraction of fVIIai bound to TF (fVIIai−TF) was the difference between observed fXa and the fXa activity in the reaction with no inhibitor [(fVIIai−TF) = 1 − fXa with inhibitor/fXa without inhibitor]. It was essential that the concentration of fVIIai was at least 10-fold greater than TF so that free fVIIai approximated total fVIIai. The data were plotted as Hill-type plots as described (*28*). In all cases, the concentration of dimeric fVIIai is represented in the Hill-type plots as the concentration of fVIIai sites. This allowed direct comparison of protein efficacy on a weight basis.

Preparation of TF−Proteoliposomes. TF−proteoliposomes were prepared according to published methods (*30*, *31*). Two different types of preparations were made. One was comprised of 20:50:30 PS:PC:phosphatidylethanolamine (PE), and the other was similar but contained 1% *N*-((6-(biotinoyl)amino)hexanoyl)- 1,2-dihexadecanoyl-*sn*-glycero-3-phosphoethanonamine (w/w, biotinyl-PE; Molecular Probes, Eugene, OR). Phospholipids were dispensed and mixed in glass tubes and dried first under a stream of argon and then under high vacuum for 2 h. They were resuspended in TBS containing 100 mM octyl β-D-glucopyranoside (Sigma) at a 15:1 octyl β-D-glucopyranoside:phospholipid molar ratio. TF was added to a ratio of 0.00172:1 (TF:phospholipids, w/w), and the solution was incubated at 37 °C for 2 h. The preparations were then dialyzed against four changes of 1000× volumes of TBS over 4 days. The TF concentration was estimated by the concentration of fVIIa needed to saturate the activation of fX. The result corresponded well with the amount expected if one-half of the TF was relipidated in the proper orientation for reaction. Phospholipid concentration was determined as previously described (*28*). The average diameter of the proteoliposomes was 100 nm, determined by dynamic light scattering using an LSA2 photon correlation spectrometer (Langley Ford Co.). This diameter, together with a phospholipid density of 1.0 g/cm^3 and a membrane thickness of 5.0 nm, provided an estimate of four TF molecules per vesicle that were in the correct orientation (*30*).

Displacement of FVIIai from TF. FVIIai-wt or dimeric fVIIai-wt with the PEG-3400 cross-linker (fVIIai-wt)$_2$−PEG (40 pM) was equilibrated with 18 pM TF (Innovin) in TBSA containing 5 mM calcium at 37 °C. The dissociation reaction was initiated by addition of 4 nM VIIa-QE. At various time points, fX (200 nM) was added to aliquots of the reaction and incubated for 60 s. This time was short relative to the time required for displacement of fVIIa(i) from TF so that the level of fVIIa−TF remained constant during the time of fXa production. FXa generation reactions were stopped by addition of 12 mM EDTA, and fXa activity was measured by chromogenic assay as described above.

Displacement of FVIIa from TF. Either fVIIa-wt or fVIIa-QE (10 pM) was added to 40 pM TF−proteoliposomes prepared as described above in TBSA containing 5 mM calcium. FVIIa and TF were allowed to reach equilibrium binding (10 min at 22 °C), and displacement was initiated by addition of fVIIai-wt (10 nM). At various time points aliquots were removed, and the remaining fVIIa-TF activity was measured as described above.

Dissociation of FVIIa from TF−Proteoliposomes. Either 9.56 nM fVIIa-wt or fVIIa-QE was added to 38.2 nM TF−proteoliposomes in TBS containing 10 mM calcium, and the reaction was allowed to reach equilibrium (10 min at 22 °C). Dissociation was initiated by addition of 38.2 nM TF−proteoliposomes that did not contain biotinyl-PE. At various time points 4 μL of SA (1 mg/mL in TBSA) was added to aliquots (20 μL) of the reaction, and incubation was continued for another 20 min to selectively precipitate the proteoliposomes containing biotinyl-PE. The aliquots were centrifuged at 12000 rpm for 5 min. Small volumes of supernatant were diluted 1000-fold in TBSA containing 5 mM calcium and warmed to 37 °C. FX was added at 100 nM and incubated for 5 min. The reaction was stopped by

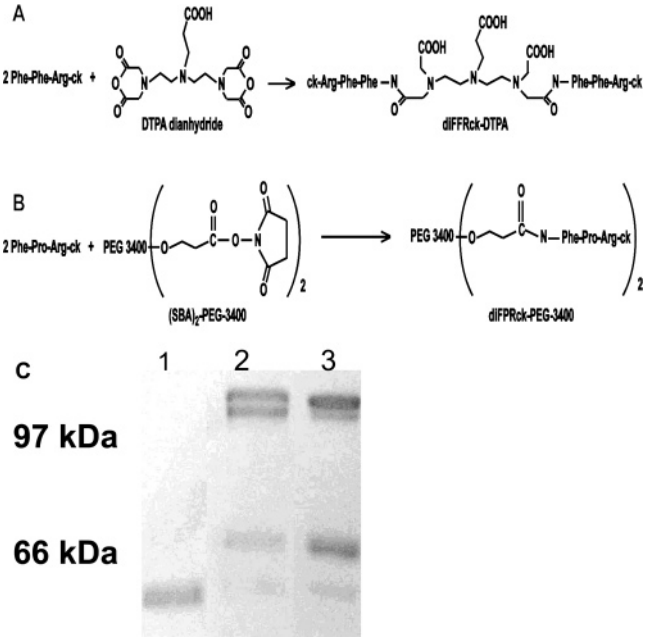

FIGURE 1: Synthesis of dimeric fVIIai. Dimeric fVIIai was made by reaction of fVIIa with a bifunctional active site inhibitor. Bifunctional active site inhibitors were produced by reaction of FFRck with DTPA dianhydride (panel A) or of FPRck and PEG-3400−$(SBA)_2$ (panel B). Products from reaction of fVIIa and diFPRck−PEG-3400 were separated by SDS−PAGE (panel C). Lanes 1, 2, and 3 correspond to fVIIa-wt alone, the product of fVIIa-wt reaction with diFPRck−PEG-3400, and the product of fVIIa-QE reaction with diFPRck−PEG-3400.

addition of EDTA to 12 mM, and fXa activity was measured as described above. FXa activity produced at various time points was compared to that obtained in a parallel experiment with no competing phospholipids. Undissociated fVIIa was expressed as a fractional activity.

Clotting Assays. FVIIa-wt (20 nM) and fVIIai were mixed in TBSA containing 6.67 mM calcium at 37 °C. At zero time, TF (1.0 μL of Innovin/112.5 μL of solution) was added. Aliquots (112.5 μL) were removed at various times, and coagulation time was measured by the hand-tilt method after addition of 37.5 μL of factor VII-deficient plasma (Sigma) that was prewarmed to 37 °C.

RESULTS

Production and Characterization of FVIIai Protein Dimers. Two homobifunctional reagents were synthesized. First, FFRck was combined with DTPA dianhydride to produce diFFRck−DTPA (Figure 1A). The cross-linker arm of this bifunctional reagent should be approximately 7 Å. Second, FPRck was combined with PEG-3400−$(SBA)_2$ to produce diFPRck−PEG-3400 with a cross-linker that should be approximately 230 Å (Figure 1B). The desired homobifunctional cross-linkers were separated from other reaction products by reverse-phase HPLC as described in Materials and Methods.

Homodimers of fVIIai-wt and fVIIai-QE were produced by combination of the respective protein with the bifunctional cross-linking reagents as described in Materials and Methods. Three major products were detected for the PEG-cross-linked protein on SDS−PAGE (Figure 1C). A doublet appeared just above the 97000 molecular weight standard. These bands were assumed to represent dimeric protein. The basis for a doublet was not determined, but virtually all recombinant preparations of fVIIa that we have analyzed show some level of a doublet that is not well resolved. A third band appeared at a mass near the 66000 molecular weight standard. This was assumed to be the fVIIai−PEG monomer. PEG has a disproportional effect on protein migration in SDS−PAGE (*32*). A fourth, very minor band migrated with the starting material and was assumed to be fVIIai produced by reaction with diisopropyl fluorophosphate. Densitometry of these bands showed 80% and 72% yields of the dimeric forms of $(fVIIai\text{-}wt)_2$−PEG and $(fVIIai\text{-}QE)_2$−PEG, respectively. SDS−PAGE and densitometric analysis of dimeric fVIIai-wt and fVIIai-QE produced from the DTPA cross-linker [$(fVIIai\text{-}wt)_2$−DPTA and $(fVIIai\text{-}QE)_2$−DPTA] suggested 33% and 21% yields, respectively (data not shown). The lower yield from the shorter cross-linking reagent may be due to steric hindrance during reaction of the cross-linker with the second molecule of fVIIa.

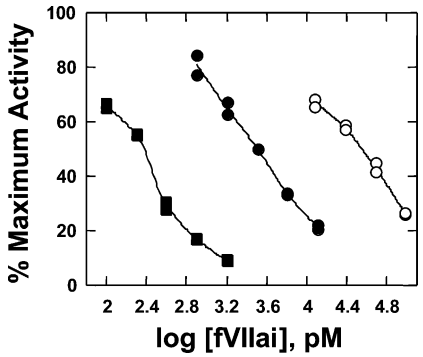

FIGURE 2: Functional inhibitory activity of $(fVIIai)_2$−DPTA. Varying amounts of fVIIai-wt (open circles), $(fVIIai\text{-}wt)_2$−DPTA (closed circles), and $(fVIIai\text{-}QE)_2$−DPTA (closed squares) were equilibrated with 20 nM fVIIa-QE and 4 pM TF (Innovin) for 60 min at 37 °C. The fraction of fVIIa-TF was determined by the two-stage fX activation assay and compared to reactions without inhibitor. Results are expressed as percent activity relative to that observed in the absence of inhibitor. Data points are from two experiments.

Functional Analysis of Dimeric FVIIai. An equilibrium competition assay (ref *18* and Materials and Methods) was used to detect the relative function of dimeric vs monomeric fVIIai. FVIIa and either $(fVIIai\text{-}wt)_2$−DPTA, $(fVIIai\text{-}QE)_2$−DPTA, or fVIIai-wt were added to TF−proteoliposomes and allowed to reach equilibrium. The relative amounts of fVIIai bound to TF were determined using the two-stage fXa generation assay and known activity level in the absence of inhibitor. Dose−response curves (Figure 2) showed that both dimeric proteins displaced fVIIa from TF more effectively than monomeric fVIIai-wt. When compared with fVIIai-wt on a weight basis, it took 175-fold less of the $(fVIIai\text{-}QE)_2$−DPTA protein preparation and 10-fold less of the $(fVIIai\text{-}wt)_2$−DPTA protein preparation to achieve 50% inhibition of TF. The presence of only 33% and 21% dimer in these preparations suggested that the true functional activity of the dimers was several times the values suggested by the comparison in Figure 2. Due to the low synthetic yield of DPTA dimers, further characterization focused on PEG-linked dimers.

The longer cross-linker arm of $(fVIIai\text{-}wt)_2$−PEG provided higher yield and function. This reagent was analyzed multiple times and at two different TF concentrations. Typical outcomes are presented in Figure 3A. The degree of enhanced

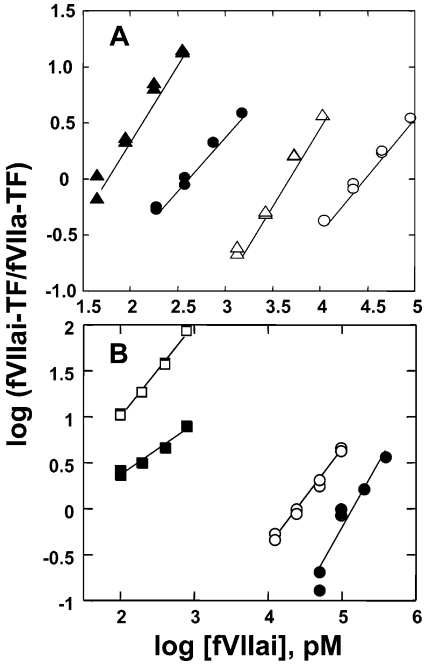

FIGURE 3: Functional inhibitory activity of $(fVIIai)_2$−PEG. Panel A: $(FVIIai\text{-}wt)_2$−PEG. Varying amounts of fVIIai-wt (open symbols) and $(fVIIai\text{-}wt)_2$−PEG (closed symbols) were equilibrated with 20 nM fVIIa-QE (circles) or 40 nM fVIIa-wt (triangles) and 18 pM TF (Innovin) for 60 min at 37 °C. The fraction of fVIIa−TF was determined by the two-stage fX activation assay and compared to fX activation without inhibitor. The results are presented as a Hill plot calculated as described in Materials and Methods. Data from two experiments for each titration are shown. Panel B: $(FVIIai\text{-}QE)_2$−PEG. Varying amounts of fVIIai-wt (circles) and dimeric fVIIai-QE (squares) were equilibrated with 20 nM fVIIa-QE (open symbols) or 100 nM fVIIa-QE (closed symbols) and 4 pM TF (Innovin) for 60 min at 37 °C. The fraction of fVIIa−TF was determined by the two-stage fX activation assay. Results are presented in the form of the Hill-type plot described in Materials and Methods. Data are from two experiments.

function of dimeric protein can be estimated by the difference in concentration needed to displace a competing protein from TF. This is obtained by horizontal comparisons in Figure 3A. A convenient point of comparison occurs where half of the competing ligand has been displaced (vertical axis = 0, Figure 3A). When 40 nM fVIIa-wt was used as the competing protein, the difference between monomer and dimer was 77-fold (Figure 3A, circles). When 20 nM fVIIa-QE was used as the competing protein, the displacement of the titration curves was 82-fold (Figure 3A, triangles). The results also illustrated the relative function of fVIIa-QE vs fVIIa-wt. Once again, at half displacement (vertical axis = 0), it required 14 times more fVIIai-wt to displace 20 nM fVIIa-QE as to displace 40 nM fVIIa-wt (compare titrations with open symbols, Figure 3A), consistent with a 28-fold greater function of fVIIa-QE over fVIIa-wt. For titrations with $(fVIIai\text{-}wt)_2$−PEG, it required 16 times higher concentration to displace 20 nM fVIIa-QE as 40 nM fVIIa-wt (compare titrations with solid symbols, Figure 3A), indicating a 32-fold higher function of fVIIa-QE. Earlier studies by several methods indicated a 25−40-fold advantage of fVIIa-QE over fVIIa-wt (*18*, *28*). The similarity of outcome for comparison of fVIIa-QE vs fVIIa-wt provided strong evidence that the analysis methods used to describe these protein−membrane assemblies and theoretical interpretation of the results were accurate.

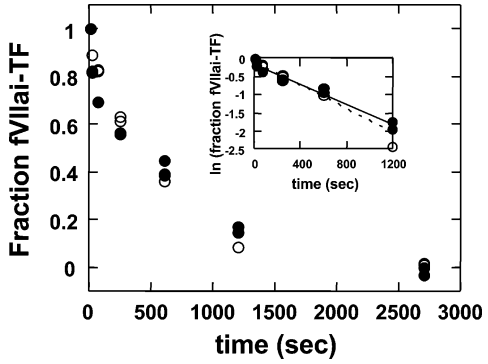

FIGURE 4: Displacement of fVIIai from TF. FVIIai-wt (open circles) or $(fVIIai\text{-}wt)_2$−PEG ((closed circles, 40 pM) was equilibrated with 18 pM TF (Innovin) for 5 min at 37 °C. Dissociation was initiated by addition of 4 nM fVIIa-QE. At various time points, aliquots were removed, and fVIIa−TF was determined by the two-stage fX activation assay. The fraction of fVIIai−TF was calculated from the difference between activity obtained in the presence and absence of inhibitor. Time corresponds to the incubation time prior to fX addition. Data from two experiments are shown. Inset: A first-order dissociation rate plot of the data.

Using similar conditions, $(fVIIai\text{-}QE)_2$−PEG was so effective that its relative function was difficult to estimate (Figure 3B). The lowest concentration of $(fVIIai\text{-}QE)_2$−PEG used (100 pM, expressed as the concentration of monomer) inhibited 90% of 20 nM fVIIa-QE function (Figure 3B). Use of lower concentrations of inhibitor was not possible because free protein no longer approximated total protein. Consequently, inhibition was repeated at a higher level of active protein (100 nM fVIIa-QE). Even under these conditions, the lowest concentration of $(fVIIai\text{-}QE)_2$−PEG produced 60% inhibition. The observed 5-fold shift in the Hill plot for both $(fVIIai\text{-}QE)_2$−PEG and fVIIai-wt was expected for a 5-fold increase of competitor (fVIIa), suggesting that the amount of free inhibitor in both experiments approximated total inhibitor so that the conditions for an accurate comparison were satisfied. Both results (Figure 3B) suggested that $(fVIIai\text{-}QE)_2$−PEG was about 1600-fold more effective than fVIIai-wt. In several other comparison titrations, the enhancement ranged from 900- to 2500-fold. Since dimeric protein represented about 72% of total protein in this preparation, an average of 1600-fold enhancement may underestimate the true function of $(fVIIai\text{-}QE)_2$−PEG.

Dissociation Rate of Dimeric FVIIai from TF. Two methods were used to measure dissociation of fVIIai or fVIIa from TF and/or proteoliposome. The first is referred to as displacement. In this case, a large excess of fVIIai or fVIIa is added to trap TF as it became available. The second method is referred to as dissociation and is achieved by trapping the dissociated fVIIa or fVIIai as it comes off of the membrane−TF particle. These two methods gave very different results.

For displacement (Figures 4 and 5A), the protein to be displaced was first bound to TF−proteoliposomes. At zero time, a large excess of competitor was added, and dissociation of the initially bound protein was measured by activity. The level of competitor used was saturating in that higher concentrations had no further effect on the rate of dissociation. Under these conditions, dimeric and monomeric forms of fVIIai were displaced from TF at almost exactly the same rate (Figure 4). The large excess of trapping protein produced an irreversible reaction allowing analysis by a first-order rate

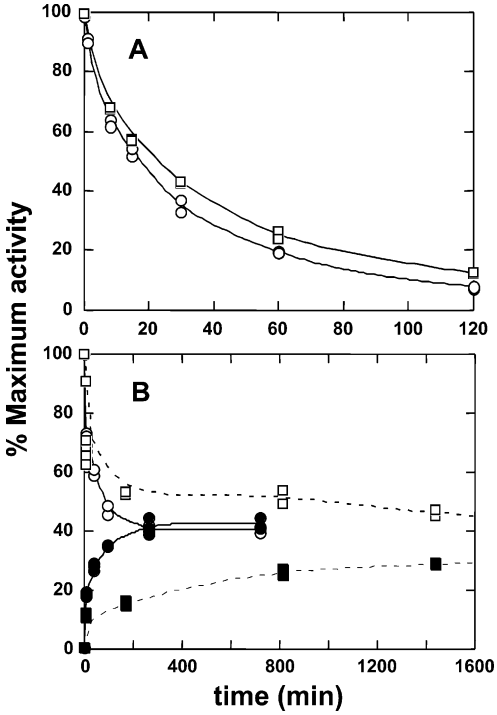

FIGURE 5: Displacement vs dissociation of fVIIa from TF−proteoliposomes. Panel A: Displacement. Either fVIIa-wt (open circles, 10 pM) or fVIIa-QE (open squares, 10 pM) was equilibrated with TF (40 pM)−proteoliposomes (PS:PC:PE, 20:50:30) for 10 min at 22 °C. Displacement was initiated by addition of fVIIai-wt (10 nM). At various time points, aliquots were removed and fVIIa−TF activity was measured by the two-stage fX activation assay. Percent maximal fVIIa−TF was calculated by comparison to a similar mixture without inhibitor. Time corresponds to incubation time prior to fX addition. Data from two experiments are shown. Panel B: Dissociation. FVIIa-wt (circles) or fVIIa-QE (squares) (9.56 nM) was preequilibrated with TF (38.2 nM)−proteoliposomes for 10 min at 22 °C. TF−proteoliposomes either contained (closed symbols) or did not contain (open symbols) 1% biotinylated PE. Dissociation was initiated by addition of appropriate TF (38.2 nM)−proteoliposomes with which fVIIa variants had not been equilibrated. At various time points SA was added to an aliquot of the reaction. After incubation for 20 min, the solution was centrifuged, selectively precipitating proteoliposomes containing biotinyl-PE. FVIIa−TF in the supernatant was measured by the two-stage fX activation assay. Percent of maximum fVIIa−TF was calculated by comparison to a control reaction that did not contain competing proteoliposomes. Time corresponds to incubation time prior to SA addition. Data from two experiments are shown.

plot (Figure 4, inset). Rate constants for dissociation of $(fVIIai\text{-}wt)_2$−PEG and fVIIai from proteoliposomes by fVIIa were 0.0014 and 0.0016 s^{-1}, respectively. The reverse experiment, displacement of fVIIa-wt from TF by addition of excess fVIIai, was 3−4 times faster than displacement of fVIIai-wt, consistent with the higher TF affinity of fVIIai (data not shown).

Previous studies showed that fVIIa-wt and fVIIa-QE had identical affinity in protein contact with TF but differed substantially with respect to their relative affinities for phospholipid membranes (*18*). If this relationship applied to monomeric vs dimeric fVIIa(i), then the two types of high-affinity proteins (dimers and site mutants) should show similar properties. This was found to be the case. Displacement of fVIIa-wt and fVIIa-QE from TF−proteoliposomes was conducted by the mechanism described in Figure 4 except that progress of the reaction was followed by loss of fVIIa−TF activity. The results (Figure 5A) showed similar displacement rates for both proteins. While the actual rate constants for the two experiments were not directly comparable since the displacement experiments in Figures 4 and 5 used different TF−proteoliposome preparations and were conducted at different temperatures, the results were consistent. That is, displacement of fVII variants from TF by addition of an excess of competing protein gave similar rates for proteins with very different membrane-binding affinities. Similar dissociation rates for monomeric vs dimeric forms of fVIIai (Figure 4) as well as for fVIIa-QE and fVIIa-wt (Figure 5A) suggested that protein−protein contact of fVIIai dimer with TF was not altered. These properties were rationalized by the two-stage dissociation process described below.

True dissociation of fVIIa from TF−proteoliposomes was measured by trapping the dissociated protein. Subsaturation levels of VIIa-wt or VIIa-QE were preequilibrated with TF−proteoliposomes, and dissociation was monitored by addition of competing TF−proteoliposomes containing 1% biotinyl-PE. At various time points, the TF−proteoliposomes containing 1% biotinyl-PE were precipitated with SA, and the fVIIa that remained bound to TF−proteoliposomes without biotinyl-PE was measured. The inverse experiment involved initial binding of the fVIIa to the vesicles containing biotinyl-PE with measurement of fVIIa appearance in the supernatant. Both experiments showed similar dynamics and reached the same equilibrium value when fVIIa-wt was used. The equilibrium point was only slightly below the theoretical value of 50% (Figure 5B), indicating nearly ideal conditions in this experiment and that biotinyl-PE did not influence protein−membrane binding. The competing TF was not present in excess so that the reaction was reversible, and first-order rate plots were not used. However, the rate at which the reaction approached equilibrium was qualitatively similar to the rate of displacement by excess fVIIai (Figure 5A), suggesting similar affinities.

In contrast to fVIIa-wt, fVIIa-QE showed multiphase dissociation with an initial rapid dissociation and subsequent slower rate. The reactions had not reached equilibrium at 52 h (Figure 5B). This experiment was repeated with a different preparation of TF−proteoliposomes with similar outcome. Due to an extremely slow dissociation, results for dimeric fVIIai are not shown. This very slow dissociation of fVIIa-QE from TF−proteoliposomes was rationalized by the two-stage dissociation process described below.

Dynamics of Anticoagulation. An in vitro coagulation model demonstrated a unique property of anticoagulation by fVIIai that may be related to the association/dissociation properties described above. Different amounts of fVIIai-wt or fVIIai-QE were premixed with 20 nM fVIIa-wt. To simulate TF exposure from injury, TF−proteoliposomes were added at zero time. Aliquots were removed at various time points, and anticoagulation was detected by an increase in clotting time of factor VII-deficient human plasma (Figure 6). After 1 min, fVIIai appeared to be a poor anticoagulant with only a sight increase in clotting time. Low anticoagulation after a short time may result from fVIIa assembly with TF at or near the diffusional limit. In fact, assembly in this assay was so rapid that timed stages were difficult to estimate (*18*). The properties of particle diffusion would therefore dominate the early stages of this reaction so that enzyme (fVIIa) would bind to TF as well as inhibitor. However, as

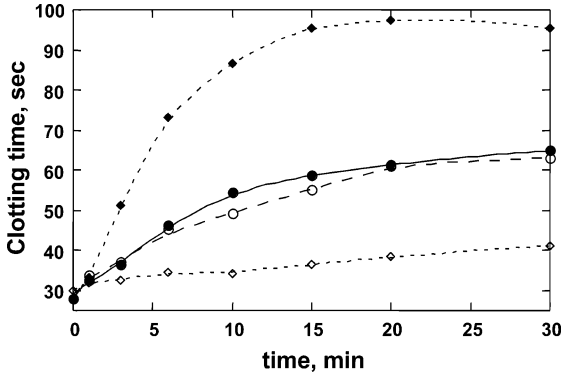

FIGURE 6: Dynamics of fVIIai inhibition. FVIIa-wt (20 nM) and varying amounts fVIIai were mixed in TBSA containing 6.67 mM calcium at 37 °C. At zero time, 18 pM TF (Innovin) was added. At various times, aliquots were removed. Coagulation was initiated by addition of factor VII-deficient plasma, and coagulation time was measured by the hand-tilt method. Time on the horizontal axis refers to incubation before plasma addition. The fVIIai species and concentrations used were fVIIai-wt (10 nM, open circles; 4.0 nM, open diamonds) and fVIIai-QE (0.4 nM, closed circles; 3.8 nM, closed diamonds).

competition binding approached equilibrium, the higher affinities of fVIIai variants such as fVIIai-QE and of dimeric proteins would become the dominant features of the reaction. At 0.4 nM fVIIai-QE and 10 nM fVIIai, the clotting time increased until about 20 min. Similar delay in onset of anticoagulation was obtained for all competing proteins, fVIIai-wt, fVIIai-QE (Figure 6), or (fVIIai-QE)$_2$−PEG (not shown). The final equilibrium showed a 25-fold difference between fVIIai-QE and fVIIai-wt, similar to the difference reported in earlier studies (*18*). Comparison at similar concentrations (4 nM fVIIai-wt and 3.8 nM fVIIai-QE) also emphasized the enhanced function of fVIIai-QE.

DISCUSSION

Excess TF exposure is thought to be common to several disease states and to traumas such as acute coronary syndromes (*33*−*36*), sepsis (*37*−*39*), disseminated intravascular coagulation (*40*), antiphospholipid syndrome (*41*), sickle cell anemia (*42*), cancer (*43*−*46*), and vascular damage. TF has been implicated in promotion of tumor angiogenesis (*47*), which therapeutic TF inhibition may attenuate (*48*). Consequently, the therapeutic implications of TF inhibitors may be substantial. Use of fVIIai may be limited by cost of production, a challenge that could be overcome by use of mutant forms of fVIIai that have higher membrane affinity and by use of dimeric molecules that provide multiple simultaneous binding sites.

This study described the production and properties of two forms of dimeric fVIIai. The DPTA cross-linker provided a spacer arm of approximately 7 Å and the PEG-3400 cross-linker, a spacer arm of approximately 230 Å. The DPTA dimer gave a relatively low yield of product. Although far superior to monomeric fVIIai-wt, the DPTA dimer also appeared to have lower function than the PEG dimer. This may arise from geometric constraints imposed by the short linker arm that interfere with simultaneous membrane binding by both proteins. The maximum impact observed in this study, greater than a 1600-fold enhancement over fVIIai-wt monomer, was achieved for a dimer of a mutant fVIIa molecule that had high membrane affinity. The wild-type dimer gave a 75-fold enhancement over monomer. These values may be underestimates of actual dimer function as the preparations contained only 70−80% dimer.

Although remarkable, a 75-fold increase of function for the (fVIIai-wt)$_2$−PEG molecule was much less than the theoretical outcome for simultaneous binding to two TF molecules. While the reported binding constants of fVIIa and TF vary, most K_D values are 10^{-9} M or lower. Thus, theoretical enhancement for simultaneous binding to two TF molecules would be $\geq 10^9$. Simultaneous binding of dimeric fVIIai-wt to TF and to a second site on the membrane also provides a very large increase in function. Given a K_D for fVIIa-wt to membrane of about 10^{-6} M (*18*), the theoretical enhancement for simultaneous membrane association by two fVIIai molecules in the dimer would be 10^6. Thus, while functional enhancements of dimeric proteins were prodigious, the magnitude was well below the theoretical maximum and did not offer a clear correlation with either protein−protein or protein−membrane interaction. The mechanism of enhanced function could arise from either interaction, but with much less than theoretical free energy of association.

Additional effects of protein modification by PEG include an increased circulation lifetime and reduced antigenic properties (*32*, *49*). A previous study showed that attachment of PEG-3400 to fVIIai resulted in 2.6-fold longer circulation lifetime in the mouse (*32*). (FVIIai-wt)$_2$−DPTA had a 1.6-fold longer circulation half-time in the mouse than monomeric fVIIai (data not shown). Consequently, the fVIIai dimer that was cross-linked by PEG-3400 should have a severalfold longer circulation lifetime than monomeric fVIIai.

The kinetics of association and dissociation of fVIIa(i) from TF−proteoliposomes provided insight into the possible mechanism of fVIIa(i) interaction with TF. A surprising finding was that, despite a large increase in equilibrium binding affinity for TF−proteoliposomes, (fVIIai-wt)$_2$−PEG and fVIIa(i)-QE were displaced from TF at similar rates by excess competing ligand. In contrast, true dissociation of fVIIa(i) from TF−proteoliposomes differed greatly for these molecules. A related property may exist in anticoagulation. FVIIai was a very poor inhibitor of coagulation right after initiation of reaction but became highly effective with time. We suggest that these properties are best explained by the two-stage association/dissociation reaction shown in Figure 7. The first step of dissociation consists of protein−protein separation while both proteins remain membrane-bound. For displacement by a competing ligand, all vacant TF molecules are immediately filled so that recapture of fVIIa(i) before dissociation from the membrane particle is not possible (Figure 7, top diagram). Consequently, displacement is limited entirely by protein−protein affinity. Dimeric forms of fVIIai as well as mutants with high membrane affinity have the same affinity for TF so that displacement proceeds at the same rate for all proteins (Figures 7, top, 4, and 5A).

For true dissociation, initial separation of fVIIa(i) from TF on the membrane can be followed by recapture by another TF molecule before the fVIIa(i) has a chance to dissociate from the membrane (Figure 7, bottom). Dimeric proteins and high-affinity mutants with longer residence times on the membrane would be more likely to be recaptured by vacant tissue factor molecules. Recapture efficiency increases as the number of vacant TF molecules increases so that the rate of fVIIa(i) dissociation slows as TF sites become empty.

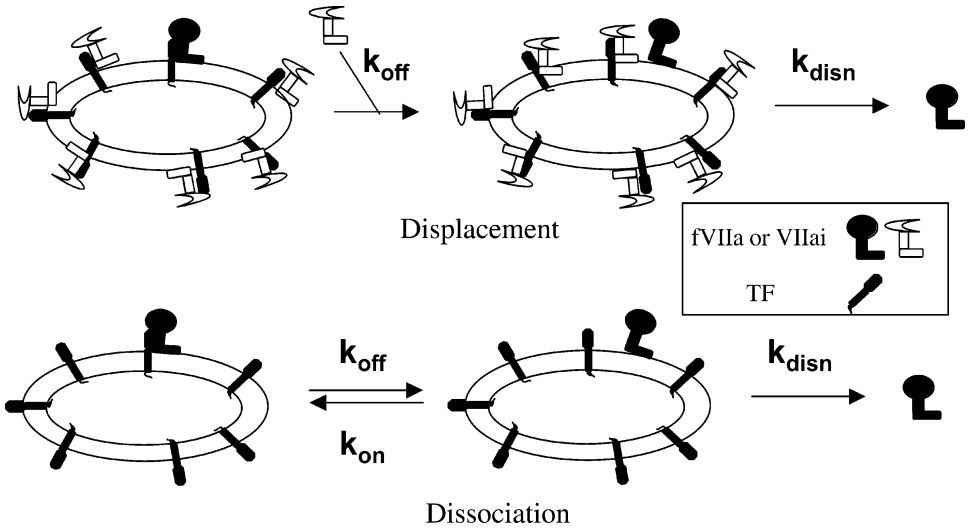

FIGURE 7: Illustration of displacement (top) and dissociation (bottom) of fVIIa(i) from TF.

Eventually, proteins with high membrane affinity can appear to stop dissociating altogether (Figure 5B, fVIIa-QE at long times) due to efficient recapture by TF on the same particle.

Previous kinetic experiments of fVIIa and TF have shown similar results with different dissociation rates for competitor displacement vs dilution-jump experiments (*50*). This difference was described as an indication of cooperative binding of fVIIa to TF and has been supported by binding experiments using TF on cells or in reconstituted liposomes that yield nonlinear Eadie−Hofstee plots (*30*) and sigmoidal binding isotherms (*51*). It does not appear that the recapture mechanism was considered.

Cooperativity did not appear to provide an adequate explanation for the results in Figures 4 and 5. For example, cooperative interaction involves protein−protein contacts, and the enhanced and dimeric proteins appeared to be unaltered in this property. Consequently, we suggest that the recapture mechanism described in Figure 7 is the more likely explanation for different displacement vs dissociation rates.

While extrapolation from one system to another must be made with caution, we suggest that the mechanism presented in Figure 7 should be considered for the earlier studies of fVIIa(i) dissociation from cell surfaces as well. That this explanation is possible was illustrated by different apparent dissociation or displacement rates of ligand or substrate from receptors such as a hapten and IgE (*52*) or for lipoprotein lipase and heparin (*53*). These receptors and/or enzymes function independent of each other so that cooperative action could not explain the result. Experimental kinetic analysis and modeling of alkaline phosphatase, a monomeric, noncooperative enzyme immobilized in the *Escherichia coli* periplasm, yielded nonlinear Eadie−Hofstee plots that were due to efficient capture/recapture of substrate (*54*). These properties were recently reviewed (*55*). Thus, efficient capture/recapture of fVIIa by TF (Figure 7) may be a general property that applies to many states of multiple receptors or enzymes per particle.

A related mechanism may explain the delay in onset of anticoagulation by fVIIai (Figure 6). Earlier studies suggested that association of fVIIa(i) with TF occurred at the rate of diffusion and particle collision (*18*). As a result, sudden appearance of TF in the circulation system due to injury would provide equal association rates for fVII, fVIIa, and any form of fVIIai. The outcome would be relatively poor inhibition by fVIIai. However, with time the two-stage association/dissociation reaction would establish equilibrium binding with competition based on the overall equilibrium binding constant. If this description were applicable in vivo, initial injury with TF exposure to the blood may allow initial blood clotting to occur despite the presence of fVIIai. This may be sufficient to stop bleeding. Slow displacement by higher affinity mutants of fVIIai might eliminate extended coagulation. This description may fit the reported anticoagulation properties of fVIIai in several animal models where fVIIai was shown to limit platelet deposition while paradoxically limiting blood loss as well (*21*, *22*, *24*). Appearance of anticoagulation with dissociation (see Figure 5B) may agree with in vivo anticoagulation properties (*56*). FVIIai might be described as a "delayed action" anticoagulant, a clear contrast with anticoagulants such as heparin that display instant anticoagulation.

FVIIai was recently tested in a phase II clinical trial as a heparin replacement following balloon angioplasty (*57*). Combined fVIIai/low dose heparin did not appear to offer significant advantage over heparin alone. However, as described above and in Figure 6, fVIIai may not be a good heparin replacement. The instantaneous anticoagulation of heparin may be superior for countering intense procoagulation conditions, and the advantage of fVIIai may occur at later times or in other situations. Future studies may find that fVIIai is ideal for some types of therapy while heparin is superior for others.

Overall, dimeric fVIIai and especially dimers of mutant proteins with enhanced membrane affinity offered an opportunity to study the mechanism of fVIIai interaction with membrane and TF. They may offer unique opportunities to investigate the state of TF on intact cells and may also offer therapeutic agents at reasonable cost. Further work is needed to define the conditions best served by the unique anticoagulation of these proteins.

REFERENCES

1. Morrissey, J. H., Macik, B. G., Neuenschwander, P. F., and Comp, P. C. (1993) Quantitation of activated factor VII levels in plasma using a tissue factor mutant selectively deficient in promoting factor VII activation, *Blood 81*, 734−744.

2. Nelsestuen, G. L., Shah, A. M., and Harvey, S. B. (2000) Vitamin K-dependent proteins, *Vitam. Horm. 58*, 355−389.
3. Kelley, R. F., Costas, K. E., O'Connell, M. P., and Lazarus, R. A. (1995) Analysis of the factor VIIa binding site on human tissue factor: effects of tissue factor mutations on the kinetics and thermodynamics of binding, *Biochemistry 34*, 10383−10392.
4. Waxman, E., Ross, J. B., Laue, T. M., Guha, A., Thiruvikraman, S. V., Lin, T. C., Konigsberg, W. H., and Nemerson, Y. (1992) Tissue factor and its extracellular soluble domain: the relationship between intermolecular association with factor VIIa and enzymatic activity of the complex, *Biochemistry 31*, 3998−4003.
5. Persson, E. (1997) Characterization of the interaction between the light chain of factor VIIa and tissue factor, *FEBS Lett. 413*, 359−363.
6. Dickinson, C. D., Kelly, C. R., and Ruf, W. (1996) Identification of surface residues mediating tissue factor binding and catalytic function of the serine protease factor VIIa, *Proc. Natl. Acad. Sci. U.S.A. 93*, 14379−14384.
7. Butenas, S., Lawson, J. H., Kalafatis, M., and Mann, K. G. (1994) Cooperative interaction of divalent metal ions, substrate, and tissue factor with factor VIIa, *Biochemistry 33*, 3449−3456.
8. Neuenschwander, P. F., and Morrissey, J. H. (1994) Roles of the membrane-interactive regions of factor VIIa and tissue factor. The factor VIIa Gla domain is dispensable for binding to tissue factor but important for activation of factor X, *J. Biol. Chem. 269*, 8007−8013.
9. Komiyama, Y., Pedersen, A. H., and Kisiel, W. (1990) Proteolytic activation of human factors IX and X by recombinant human factor VIIa: effects of calcium, phospholipids, and tissue factor, *Biochemistry 29*, 9418−9425.
10. Edgington, T. S., Mackman, N., Brand, K., and Ruf, W. (1991) The structural biology of expression and function of tissue factor, *Thromb. Haemostasis 66*, 67−79.
11. Giesen, P. L., Rauch, U., Bohrmann, B., Kling, D., Roque, M., Fallon, J. T., Badimon, J. J., Himber, J., Riederer, M. A., and Nemerson, Y. (1999) Blood-borne tissue factor: another view of thrombosis, *Proc. Natl. Acad. Sci. U.S.A. 96*, 2311−2315.
12. Tay, S. P., Cheong, S. K., and Boo, N. Y. (2003) Circulating tissue factor, tissue factor pathway inhibitor and D-dimer in umbilical cord blood of normal term neonates and adult plasma, *Blood Coagulation Fibrinolysis 14*, 125−129.
13. Falati, S., Liu, Q., Gross, P., Merrill-Skoloff, G., Chou, J., Vandendries, E., Celi, A., Croce, K., Furie, B. C., and Furie, B. (2003) Accumulation of tissue factor into developing thrombi in vivo is dependent upon microparticle P-selectin glycoprotein ligand 1 and platelet P-selectin, *J. Exp. Med. 197*, 1585−1598.
14. Balasubramanian, V., Grabowski, E., Bini, A., and Nemerson, Y. (2002) Platelets, circulating tissue factor, and fibrin colocalize in ex vivo thrombi: real-time fluorescence images of thrombus formation and propagation under defined flow conditions, *Blood 100*, 2787−2792.
15. Nutescu, E., and Singh-Khalsa, M. (2004) Treatment of venous thromboembolism: challenging the unfractionated heparin standard, *Pharmacotherapy 24*, 127S−131S.
16. Levine, M. N., Raskob, G., Beyth, R. J., Kearon, C., and Schulman, S. (2004) Hemorrhagic complications of anticoagulant treatment: The Seventh ACCP Conference on Antithrombotic and Thrombolytic Therapy, *Chest 126* (3 Suppl.), 287S−310S.
17. Hirsh, J., Anand, S. S., Halperin, J. L., and Fuster, V. (2001) AHA Scientific Statement: Guide to anticoagulant therapy: heparin: a statement for healthcare professionals from the American Heart Association, *Arterioscler. Thromb. Vasc. Biol. 21*, E9-9.
18. Nelsestuen, G. L., Stone, M., Martinez, M. B., Harvey, S. B., Foster, D., and Kisiel, W. (2001) Elevated function of blood clotting factor VIIa mutants that have enhanced affinity for membranes. Behavior in a diffusion-limited reaction, *J. Biol. Chem. 276*, 39825−39831.
19. Sorensen, B. B., and Rao, L. V. (1998) Interaction of activated factor VII and active site-inhibited activated factor VII with tissue factor, *Blood Coagulation Fibrinolysis 9* (Suppl. 1), S67−S71.
20. Holst, J., Kristensen, A. T., Kristensen, H. I., Ezban, M., and Hedner, U. (1998) Local application of recombinant active-site inhibited human clotting factor VIIa reduces thrombus weight and improves patency in a rabbit venous thrombosis model, *Eur. J. Vasc. Endovasc. Surg. 15*, 515−520.
21. Ghrib, F., Leger, P., Ezban, M., Kristensen, A., Cambus, J., and Boneu, B. (2001) Anti-thrombotic and haemorrhagic effects of active site-inhibited factor VIIa in rats, *Br. J. Haematol. 112*, 506−512.
22. Soderstrom, T., Hedner, U., and Arnljots, B. (2001) Active site-inactivated factor VIIa prevents thrombosis without increased surgical bleeding: topical and intravenous administration in a rat model of deep arterial injury, *J. Vasc. Surg. 33*, 1072−1079.
23. Arnljots, B., Soderstrom, T., Ezban, M., and Hedner, U. (2000) Effect of locally-applied active site-blocked activated factor VII (ASIS) on experimental arterial thrombosis, *Blood Coagulation Fibrinolysis 11* (Suppl. 1), S145−S148.
24. Harker, L. A., Hanson, S. R., Wilcox, J. N., and Kelly, A. B. (1996) Antithrombotic and antilesion benefits without hemorrhagic risks by inhibiting tissue factor pathway, *Haemostasis 26* (Suppl. 1), 76−82.
25. Carraway, M. S., Welty-Wolf, K. E., Miller, D. L., Ortel, T. L., Idell, S., Ghio, A. J., Petersen, L. C., and Piantadosi, C. A. (2003) Blockade of tissue factor: treatment for organ injury in established sepsis, *Am. J. Respir. Crit. Care Med. 167*, 1200−1209.
26. Welty-Wolf, K. E., Carraway, M. S., Miller, D. L., Ortel, T. L., Ezban, M., Ghio, A. J., Idell, S., and Piantadosi, C. A. (2001) Coagulation blockade prevents sepsis-induced respiratory and renal failure in baboons, *Am. J. Respir. Crit. Care Med. 164*, 1988−1996.
27. Shah, A. M., Kisiel, W., Foster, D. C., and Nelsestuen, G. L. (1998) Manipulation of the membrane binding site of vitamin K-dependent proteins: enhanced biological function of human factor VII, *Proc. Natl. Acad. Sci. U.S.A. 95*, 4229−4234.
28. Harvey, S. B., Stone, M. D., Martinez, M. B., and Nelsestuen, G. L. (2003) Mutagenesis of the gamma-carboxyglutamic acid domain of human factor VII to generate maximum enhancement of the membrane contact site, *J. Biol. Chem. 278*, 8363−8369.
29. Mayer, L. D., Hope, M. J., and Cullis, P. R. (1986) Vesicles of variable sizes produced by a rapid extrusion procedure, *Biochim. Biophys. Acta 858*, 161−168.
30. Bach, R., Gentry, R., and Nemerson, Y. (1986) Factor VII binding to tissue factor in reconstituted phospholipid vesicles: induction of cooperativity by phosphatidylserine, *Biochemistry 25*, 4007−4020.
31. Mimms, L. T., Zampighi, G., Nozaki, Y., Tanford, C., and Reynolds, J. A. (1981) Phospholipid vesicle formation and transmembrane protein incorporation using octyl glucoside, *Biochemistry 20*, 833−840.
32. Stone, M., Harvey, S. B., Kisiel, W., Foster, D., and Nelsestuen, G. L. (2002) Unusual benefits of macromolecular shielding by polyethylene glycol for reactions at the diffusional limit: the case of factor VIIai and tissue factor, *Biochemistry 41*, 15820−15825.
33. Suefuji, H., Ogawa, H., Yasue, H., Kaikita, K., Soejima, H., Motoyama, T., Mizuno, Y., Oshima, S., Saito, T., Tsuji, I., Kumeda, K., Kamikubo, Y., and Nakamura, S. (1997) Increased plasma tissue factor levels in acute myocardial infarction, *Am. Heart J. 134* (2 Part 1), 253−259.
34. Wilcox, J. N., Smith, K. M., Schwartz, S. M., and Gordon, D. (1989) Localization of tissue factor in the normal vessel wall and in the atherosclerotic plaque, *Proc. Natl. Acad. Sci. U.S.A. 86*, 2839−2843.
35. Misumi, K., Ogawa, H., Yasue, H., Soejima, H., Suefuji, H., Nishiyama, K., Takazoe, K., Tsuji, I., Kumeda, K., and Nakamura, S. (1998) Comparison of plasma tissue factor levels in unstable and stable angina pectoris, *Am. J. Cardiol. 81*, 22−26.
36. Kim, H. K., Song, K. S., Park, Y. S., Yun, Y. S., and Shim, W. H. (2000) Changes of plasma tissue factor and tissue factor pathway inhibitor antigen levels and induction of tissue factor expression on the monocytes in coronary artery disease, *Cardiology 93*, 31−36.
37. Osterud, B., and Flaegstad, T. (1983) Increased tissue thromboplastin activity in monocytes of patients with meningococcal infection: related to an unfavourable prognosis, *Thromb. Haemostasis 49*, 5−7.
38. Drake, T. A., Cheng, J., Chang, A., and Taylor, F. B., Jr. (1993) Expression of tissue factor, thrombomodulin, and E-selectin in baboons with lethal *Escherichia coli* sepsis, *Am. J. Pathol. 142*, 1458−1470.
39. Todoroki, H., Nakamura, S., Higure, A., Okamoto, K., Tadeka, S., Nagata, N., Itoh, H., and Ohsato, K. (2000) Neutrophils express tissue factor in a monkey model of sepsis, *Surgery 127*, 209−216.
40. Asakura, H., Kamikubo, Y., Goto, A., Shiratori, Y., Yamazaki, M., Jokaji, H., Saito, M., Uotani, C., Kumabashiri, I., and Morishita, E. (1995) Role of tissue factor in disseminated intravascular coagulation, *Thromb. Res. 80*, 217−224.

41. Amengual, O., Atsumi, T., Khamashta, M. A., and Hughes, G. R. (1998) The role of the tissue factor pathway in the hypercoagulable state in patients with the antiphospholipid syndrome, *Thromb. Haemostasis 79*, 276−281.
42. Key, N. S., Slungaard, A., Dandelet, L., Nelson, S. C., Moertel, C., Styles, L. A., Kuypers, F. A., and Bach, R. R. (1998) Whole blood tissue factor procoagulant activity is elevated in patients with sickle cell disease, *Blood 91*, 4216−4223.
43. Lykke, J., and Nielsen, H. J. (2003) The role of tissue factor in colorectal cancer, *Eur. J. Surg. Oncol. 29*, 417−422.
44. Abdulkadir, S. A., Carvalhal, G. F., Kaleem, Z., Kisiel, W., Humphrey, P. A., Catalona, W. J., and Milbrandt, J. (2000) Tissue factor expression and angiogenesis in human prostate carcinoma, *Hum. Pathol. 31*, 443−447.
45. Koomagi, R., and Volm, M. (1998) Tissue-factor expression in human non-small-cell lung carcinoma measured by immunohistochemistry: correlation between tissue factor and angiogenesis, *Int. J. Cancer 79*, 19−22.
46. Vrana, J. A., Stang, M. T., Grande, J. P., and Getz, M. J. (1996) Expression of tissue factor in tumor stroma correlates with progression to invasive human breast cancer: paracrine regulation by carcinoma cell-derived members of the transforming growth factor beta family, *Cancer Res. 56*, 5063−5070.
47. Belting, M., Dorrell, M. I., Sandgren, S., Aguilar, E., Ahamed, J., Dorfleutner, A., Carmeliet, P., Mueller, B. M., Friedlander, M., and Ruf, W. (2004) Regulation of angiogenesis by tissue factor cytoplasmic domain signaling, *Nat. Med. 10*, 502−509.
48. Hembrough, T. A., Swartz, G. M., Papathanassiu, A., Vlasuk, G. P., Rote, W. E., Green, S. J., and Pribluda, V. S. (2003) Tissue factor/factor VIIa inhibitors block angiogenesis and tumor growth through a nonhemostatic mechanism, *Cancer Res. 63*, 2997−3000.
49. Molineux, G. (2003) Pegylation: engineering improved biopharmaceuticals for oncology, *Pharmacotherapy 23* (8 Part 2), 3S−8S.
50. Ruf, W., Miles, D. J., Rehemtulla, A., and Edgington, T. S. (1992) Cofactor residues lysine 165 and 166 are critical for protein substrate recognition by the tissue factor-factor VIIa protease complex, *J. Biol. Chem. 267*, 6375−6381.
51. Fair, D. S., and MacDonald, M. J. (1987) Cooperative interaction between factor VII and cell surface-expressed tissue factor, *J. Biol. Chem. 262*, 11692−11698.
52. Goldstein, B., Posner, R. G., Torney, D. C., Erickson, J., Holowka, D., and Baird, B. (1989) Competition between solution and cell surface receptors for ligand. Dissociation of hapten bound to surface antibody in the presence of solution antibody, *Biophys. J. 56*, 955−966.
53. Lookene, A., Chevreuil, O., Ostergaard, P., and Olivecrona, G. (1996) Interaction of lipoprotein lipase with heparin fragments and with heparan sulfate: stoichiometry, stabilization, and kinetics, *Biochemistry 35*, 12155−12163.
54. Martinez, M. B., Flickinger, M. C., and Nelsestuen, G. L. (1996) Accurate kinetic modeling of alkaline phosphatase in the *Escherichia coli* periplasm: implications for enzyme properties and substrate diffusion, *Biochemistry 35*, 1179−1186.
55. Nelsestuen, G. L., and Martinez, M. B. (1997) Steady state enzyme velocities that are independent of [enzyme]: an important behavior in many membrane and particle-bound states, *Biochemistry 36*, 9081−9086.
56. Cirillo, P., Golino, P., Ragni, M., D'Andrea, D., Calabro, P., Corcione, N., Vigorito, F., Ravera, M., and Chiariello, M. (2003) Long-lasting antithrombotic effects of a single dose of human recombinant, active site-blocked factor VII: insights into possible mechanism(s) of action, *J. Thromb. Haemostasis 1*, 992−998.
57. Kleiman, N. S., and Califf, R. M. (2000) Results from late-breaking clinical trials sessions at ACCIS 2000 and ACC 2000. American College of Cardiology, *J. Am. Coll. Cardiol. 36*, 310−325.

BI050007Z